Finite Element Formulation

Continous system

We start by considering the continous system of equations, given in the lecture as

$$\rho \frac{\partial \boldsymbol{v}}{\partial t} + \nabla p = 0 \tag{1}$$

$$\frac{1}{c^2}\frac{\nabla p}{t} + \rho \nabla \cdot \boldsymbol{v} = 0 \tag{2}$$

The normal form, provided in the lecture notes reads

$$\frac{\partial u}{\partial t} + D(f(u)) = 0 \tag{3}$$

One can quickly see, that Equations 1-(2) can be fitted into Eqaution (3) by defining

$$\boldsymbol{u} = \begin{pmatrix} \boldsymbol{v} \\ p \end{pmatrix}, D := \begin{pmatrix} \nabla\cdot & 0 \\ 0 & \nabla \end{pmatrix}, \boldsymbol{A} := \begin{pmatrix} 0 & \frac{1}{\rho} \\ \rho c^2 \boldsymbol{I} & 0 \end{pmatrix}, f(\boldsymbol{u}) = \boldsymbol{A}\boldsymbol{u} \tag{4}$$

for the particular simple 1-dimensional case of this problem, one thus gets

$$\boldsymbol{u} = \begin{pmatrix} v \\ p \end{pmatrix}, D := \begin{pmatrix} \frac{\partial}{\partial x}\cdot & 0 \\ 0 & \frac{\partial}{\partial x} \end{pmatrix}, \boldsymbol{A} := \begin{pmatrix} 0 & \frac{1}{\rho} \\ \rho c^2 & 0 \end{pmatrix} \tag{5}$$

One-dimensional discretization

All furhther considerations are restricted to the 1D-case described in Equations (3) and (5).
For the Galerkin approximation, test functions are defined as follows

$$\boldsymbol{w} = \begin{pmatrix} w1 \\ w2 \end{pmatrix} \quad \left\{ w \in H^1(\Omega),\ w = 0 \text{ on } \partial\Omega_D \right\} \tag{6}$$

One thus gets

$$(u_t, w)_{D^k} + (D(f(u)), w)_{D^k} = 0 \tag{7}$$

partial integration leads to

$$(u_t, w)_{D^k} - (f(u), D(w))_{D^k} + (f*(u), Gw)_{\partial D^k} = 0 \tag{8}$$

$$G = \begin{pmatrix} \hat{n} & 0 \\ 0 & \hat{n}\cdot \end{pmatrix} \tag{9}$$

where f^* is the so-called "numerical flux", which simply is the value for $f(u)$ taken at the interface. Since in the DG context, this value differes from one adjacent element to the other, a rule must be found to decide upo a certain value. The flux will choice and derivation of an approriate flux will be treated later.

In the 1D case, the above equation can be written as

$$(u,w)_{D^k} - (f(u), Dw)_{D^k} + f^*(u)^T \Big|_{x_k}^{x_{k+1}} \boldsymbol{I} = 0 \tag{10}$$

The problem is now discretized with a Bubnov-Galerkin scheme,so

$$w_h = \sum_{k=1}^{N} \boldsymbol{\phi_k} \mathbf{w_k} \tag{11}$$

$$u_h = \sum_{k=1}^{N} \boldsymbol{\phi_k} \mathbf{u_k} \tag{12}$$

are the approximation to the shape-function and the test-function.

In the above equations, one still has to take into account, that u consists of the two independent variables v and p. Therefor, they have to be weighted and tested independently.We can thus write:

$$w_h = \sum_{k=1}^{N} \begin{bmatrix} \phi_k^1 & 0 \\ 0 & \phi_k^2 \end{bmatrix} \cdot \begin{bmatrix} w_k^1 \\ w_k^2 \end{bmatrix} = \sum_{k=1}^{N} \boldsymbol{\phi_k} \cdot \mathbf{w_k} \tag{13}$$

$$u_h = \sum_{k=1}^{N} \begin{bmatrix} \phi_k^1 & 0 \\ 0 & \phi_k^2 \end{bmatrix} \cdot \begin{bmatrix} u_k^1 \\ u_k^2 \end{bmatrix} = \sum_{k=1}^{N} \boldsymbol{\phi_k} \cdot \mathbf{u_k} \tag{14}$$

The shape-functions $\boldsymbol{\phi_k}$ are taken as Lagrange-polynomials based on Gauss-Lobatto points. For the purpose of this report, shape-functions up to a degree of 10 have been implemented.

By inserting the above ansatz into the weak form provided in (10), on can thus derive the following matrix notation:

$$\mathbf{M\ddot{u}} + (-\mathbf{S} + \mathbf{F})\mathbf{u} = -\mathbf{F_{bound}}\mathbf{h} \text{ where e.g.} \tag{15}$$

$$\mathbf{M_{ij}} = (\boldsymbol{\phi_i}, \boldsymbol{\phi_j}) \tag{16}$$

Since $\boldsymbol{\phi_i}$ has a 2x2 matrix shape, the full $\mathbf{M}$ matrix consists of diagonal 2x2 blocks assembled through the dof numbering sheme as depicted in Figure 1. The element matrix genaration can be formaulated in matrixform as:

$$\mathbf{M_k} = \int_{D^k} \mathbf{N}\mathbf{N}^T det(\mathbf{J}) d\xi \tag{17}$$

$$\mathbf{S_k} = \int_{D^k} \mathbf{D}\mathbf{N}\mathbf{A}\mathbf{N}^T \mathbf{J}^{-1} det\mathbf{J} d\xi, \text{ where} \tag{18}$$

$$\mathbf{N} = \begin{bmatrix} \phi_k^1 & 0 \\ 0 & \phi_k^2 \\ \vdots & \vdots \\ \phi_k^n & 0 \\ 0 & \phi_k^n \end{bmatrix} \tag{19}$$

F-matrix

The derivation of the flux-matrix $\mathbf{F}$ is somewhat more difficult. We consider the last term of the wek form given in (10). Clearly the resulting matrix depends on the definition of f^*. For this report, the Lax-Friedrichs(LF) and the Hydrizable Discontinous Galerkin(HDG) flux were considered.

Lax-Friedrich flux

The Lax Friedrich flux is defined as

$$f^{*,LF}(u^+, u^-) = \frac{f(u^-) + f(u^+)}{2} + \frac{C}{2} \hat{\boldsymbol{n}}^- (u^- - u^+) \tag{20}$$

where u^- denotes the u value of the current element and u^+ denotes the u value of the neigbour.

The Flux matrix shall be exemplarily derived by looking at one elmenet k as described in Figure 2.

Left Node

$$u^+ = \begin{pmatrix} v_{k-1}^2 \\ p_{k-1}^2 \end{pmatrix}, u^- = \begin{pmatrix} v_k^1 \\ p_k^1 \end{pmatrix}, \hat{n}^- = -1 \tag{21}$$

$$f^{*,LF}(x_k) = \frac{\mathbf{A_k}\begin{pmatrix} v_k^1 \\ p_k^1 \end{pmatrix} + \mathbf{A_{k-1}}\begin{pmatrix} v_{k-1}^2 \\ p_{k-1}^2 \end{pmatrix}}{2} - \frac{C_k\begin{pmatrix} v_k^1 \\ p_k^1 \end{pmatrix} - C_{k-1}\begin{pmatrix} v_{k-1}^2 \\ p_{k-1}^2 \end{pmatrix}}{2} \tag{22}$$

$$= \frac{1}{2}(\mathbf{A_k} - C_k\mathbf{I})\begin{pmatrix} v_k^1 \\ p_k^1 \end{pmatrix} + \frac{1}{2}(\mathbf{A_{k-1}} + C_{k-1}\mathbf{I})\begin{pmatrix} v_{k-1}^2 \\ p_{k-1}^2 \end{pmatrix} \tag{23}$$

Right Node

$$u^+ = \begin{pmatrix} v_{k+1}^1 \\ p_{k+1}^1 \end{pmatrix}, u^- = \begin{pmatrix} v_k^2 \\ p_k^2 \end{pmatrix}, \hat{n}^- = 1 \tag{24}$$

$$f^{*,LF}(x_k) = \frac{\mathbf{A_k}\begin{pmatrix} v_k^2 \\ p_k^2 \end{pmatrix} + \mathbf{A_{k-1}}\begin{pmatrix} v_{k+1}^1 \\ p_{k+1}^1 \end{pmatrix}}{2} + \frac{C_k\begin{pmatrix} v_k^2 \\ p_k^2 \end{pmatrix} - C_{k-1}\begin{pmatrix} v_{k+1}^1 \\ p_{k+1}^1 \end{pmatrix}}{2} \tag{25}$$

$$= \frac{1}{2}(\mathbf{A_k} + C_k\mathbf{I})\begin{pmatrix} v_k^2 \\ p_k^2 \end{pmatrix} + \frac{1}{2}(\mathbf{A_{k+1}} - C_{k+1}\mathbf{I})\begin{pmatrix} v_{k+1}^1 \\ p_{k+1}^1 \end{pmatrix} \tag{26}$$

So as a whole, for the boundary integral in Equation (10) the following term can be derived

$$\begin{aligned} f^{*,LF}(x_{k+1}) - f^{*,LF}(x_k) =& \frac{1}{2}(\mathbf{A_k} + C_k\mathbf{I})\begin{pmatrix} v_k^2 \\ p_k^2 \end{pmatrix} + \frac{1}{2}(\mathbf{A_{k+1}} - C_{k+1}\mathbf{I})\begin{pmatrix} v_{k+1}^1 \\ p_{k+1}^1 \end{pmatrix} \\ & -\frac{1}{2}(\mathbf{A_k} - C_k\mathbf{I})\begin{pmatrix} v_k^1 \\ p_k^1 \end{pmatrix} - \frac{1}{2}(\mathbf{A_{k-1}} + C_{k-1}\mathbf{I})\begin{pmatrix} v_{k-1}^2 \\ p_{k-1}^2 \end{pmatrix} \end{aligned} \tag{27}$$

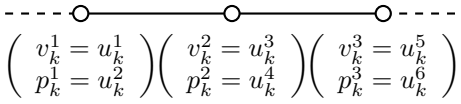

Figure 1: Dof numbering convention for the 1D-example

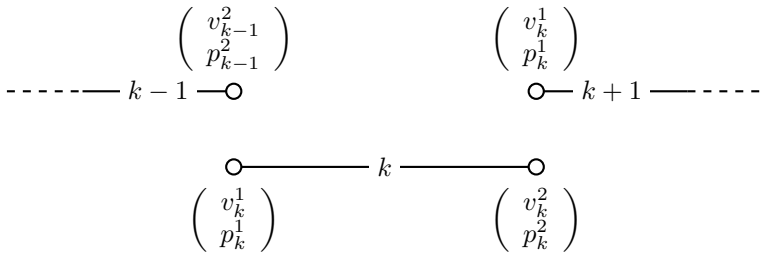

Figure 2: Element notation

Tasks

Task1

The derivation of the local Lax-Friedrich flux has been carried out above.

Task2

A formula for calculation of the timestep is provided in the lecture notes. Substitution, according to our Notation leads to:

$$\Delta t \leq K \frac{h}{p^2 c} \tag{28}$$

Here, K denotes a constant that is independent from the discretization. It depends only on the equation at hand, as well as the time integration method, and can thus be found easily by numerical experiments.

Task3

The setup for task 3 is shown in Figure 3. The simulation has been carried out with an timestep obtained by Equation (28). As Figures 4-6 show, the convergence order can be improved by using higher order polynomials, as expected. In general, the Lax-Friedrich flux deliverd slightly better results than the HDG-flux.

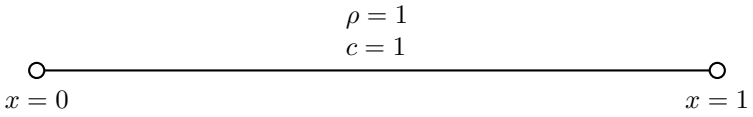

Figure 3: Setup for task 3. Both parameters ρ and c are constant in the whole domain.

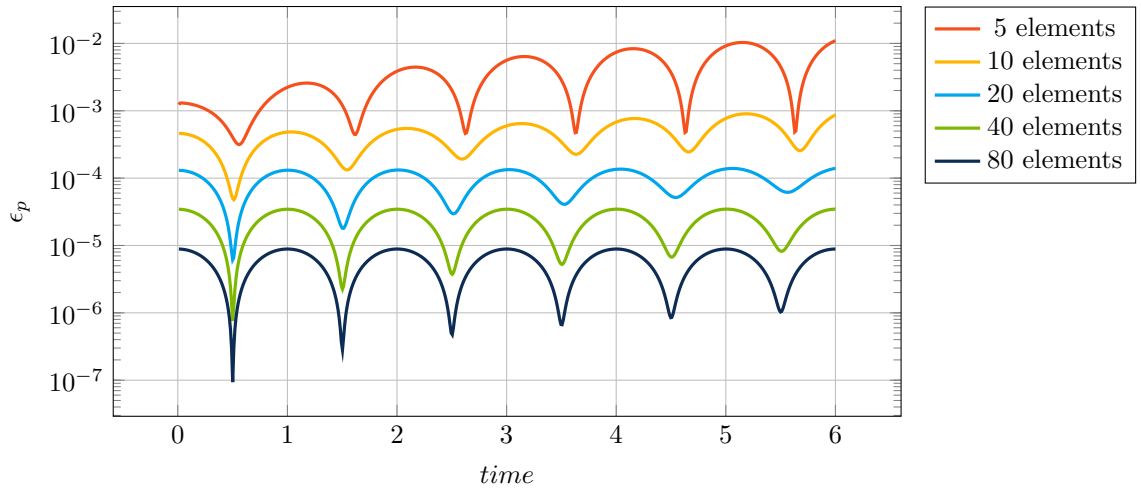

Figure 4: Development of the integral L2-error of p for the setup described in 3 from $t = 0$ to $t = 6$

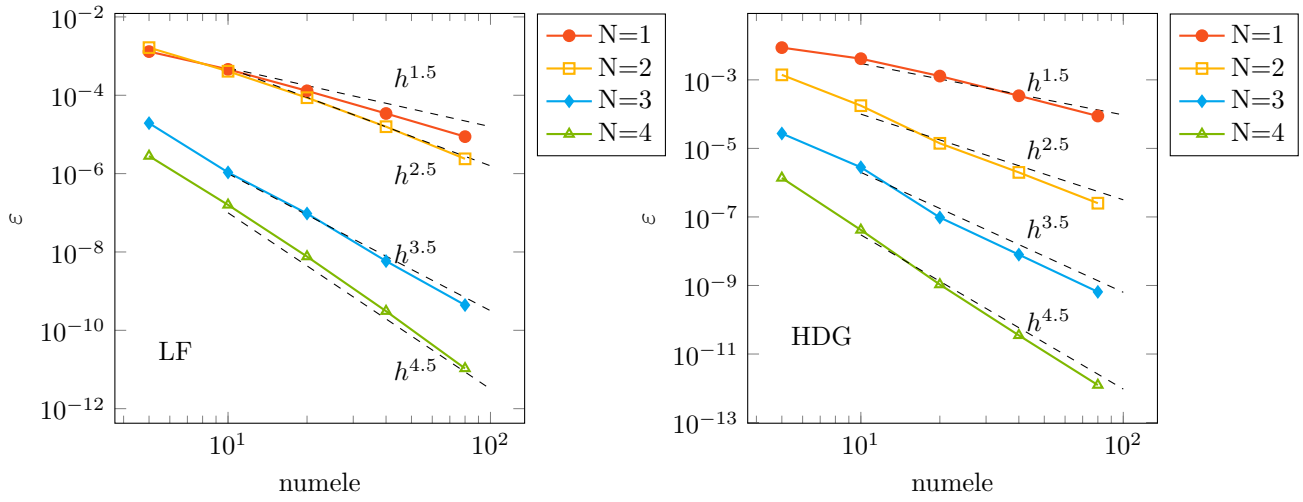

Figure 5: Setup as described in Figure 3. The L2-error is evaluated at after 10 timesteps. The timestep was 1.0e-6. In general, we can observe, that both the HDG and the LF-flux deliver statisfying results. The expected convergence order has been obtained for all polynomial degrees.

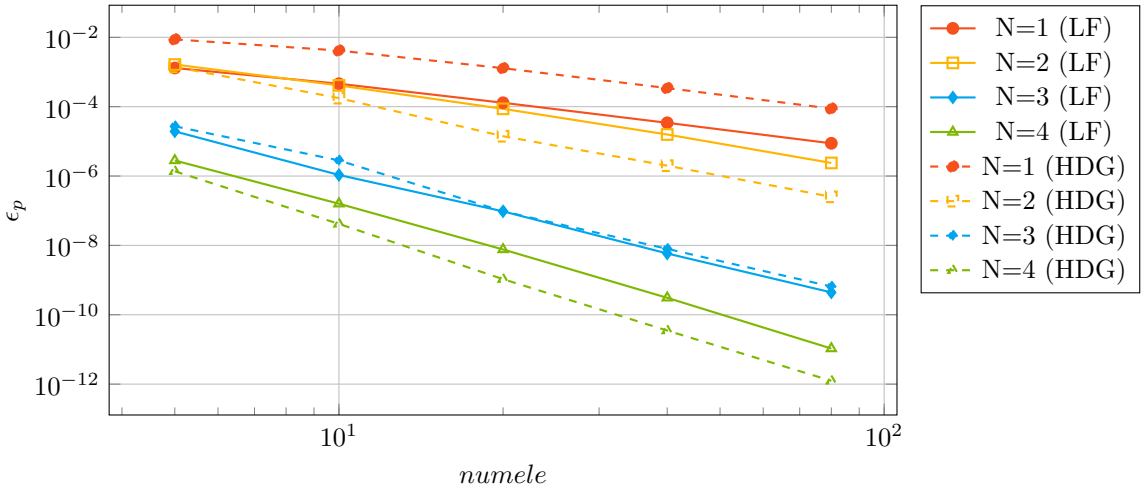

Figure 6: Comparison of LF and HDG flux for task 3. From this setup one can not really determine a superior flux.

Task4

The basic setup for task 4 is shown in Figure 8. The simulation has been carried oput with an timestep of $1e-6$. Figures 9-10 show the results for LF and HDG, both with Dirichlet and absorbing boundary conditions.

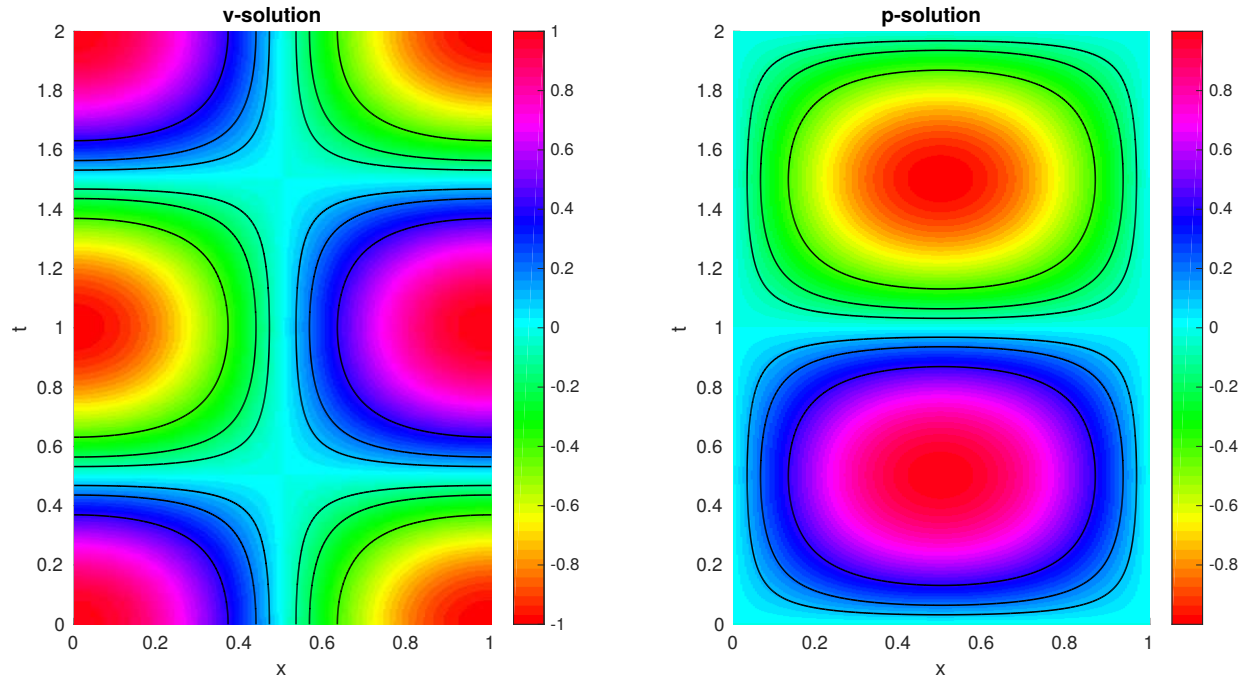

Figure 7: Setup as described in 3 with dirichlet boundary conditions. The x-axis shows the position, the y-axis the time. At perfectly periodic oscillation can be observed. For this plot 200 elements with a polymomial degree of 1 were used.

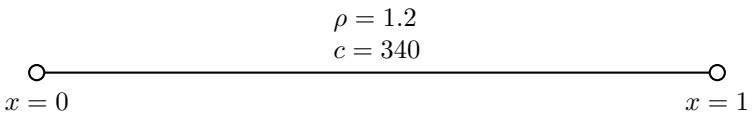

Figure 8: Setup for task 4. Both parameters ρ and c are constant in the whole domain.

Task5

The basic setup for task 5 is shown in Figure 11. Both ρ and c show a jump at $x = \frac{1}{3}$ and $x = \frac{2}{3}$ respectively.

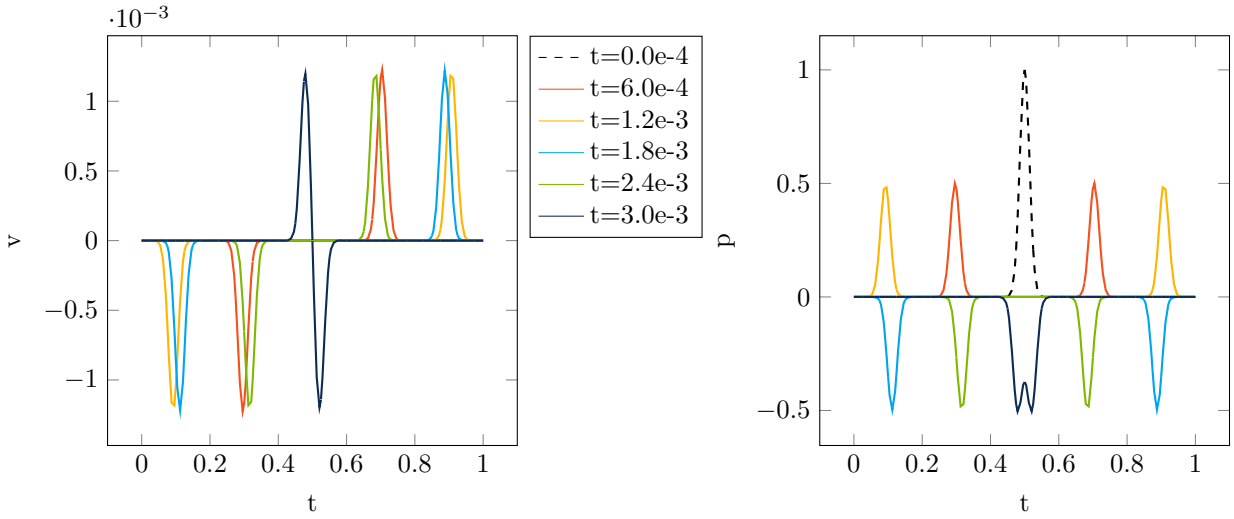

Figure 9: Setup described in Figure 8, with Dirichlet boundary conditions and a HDG-flux. There is no unphysical change in the wave form or amplitude. The setup was calculated with 40 elements of polynomial degree 4 and a timestep of 1.0e-6 in a Runge-Kutta-4 scheme.

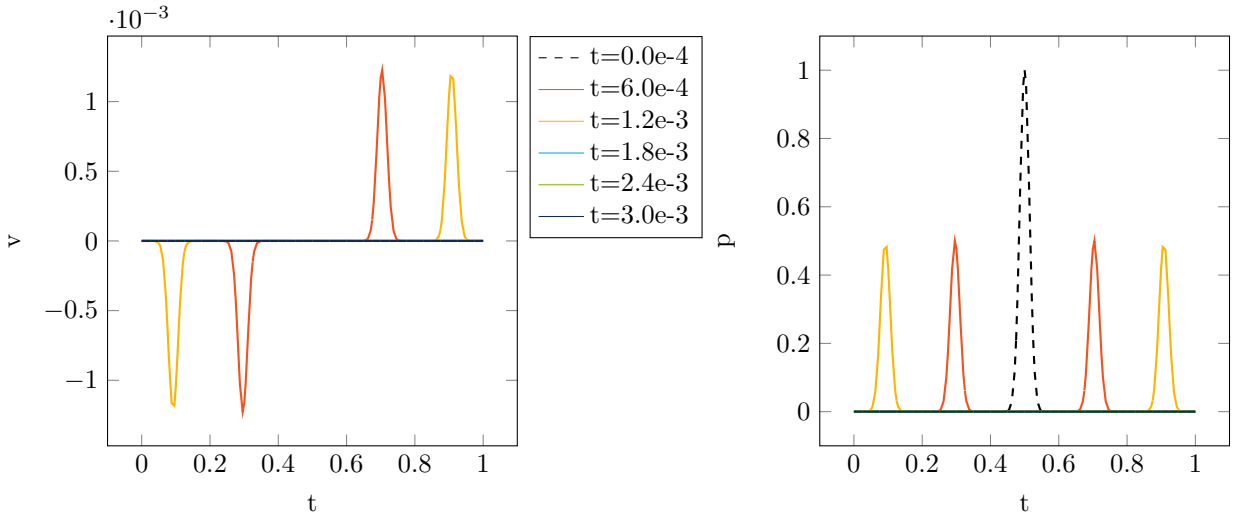

Figure 10: Setup described in Figure 8, with absorbing boundary conditions and a HDG-flux. There is no unphysical change in the wave form or amplitude, neither is anything falsely reflected at the boundary. The setup was calculated with 40 elements of polynomial degree 4 and a timestep of $\Delta t = 1.0 * 10^{-6}$ in a Runge-Kutta-4 scheme.

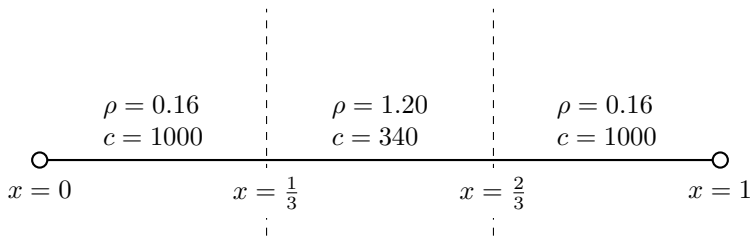

Figure 11: Setup for task 5. Both parameters ρ and c show a significant jump at $x = \frac{1}{3}$ and $x = \frac{2}{3}$.

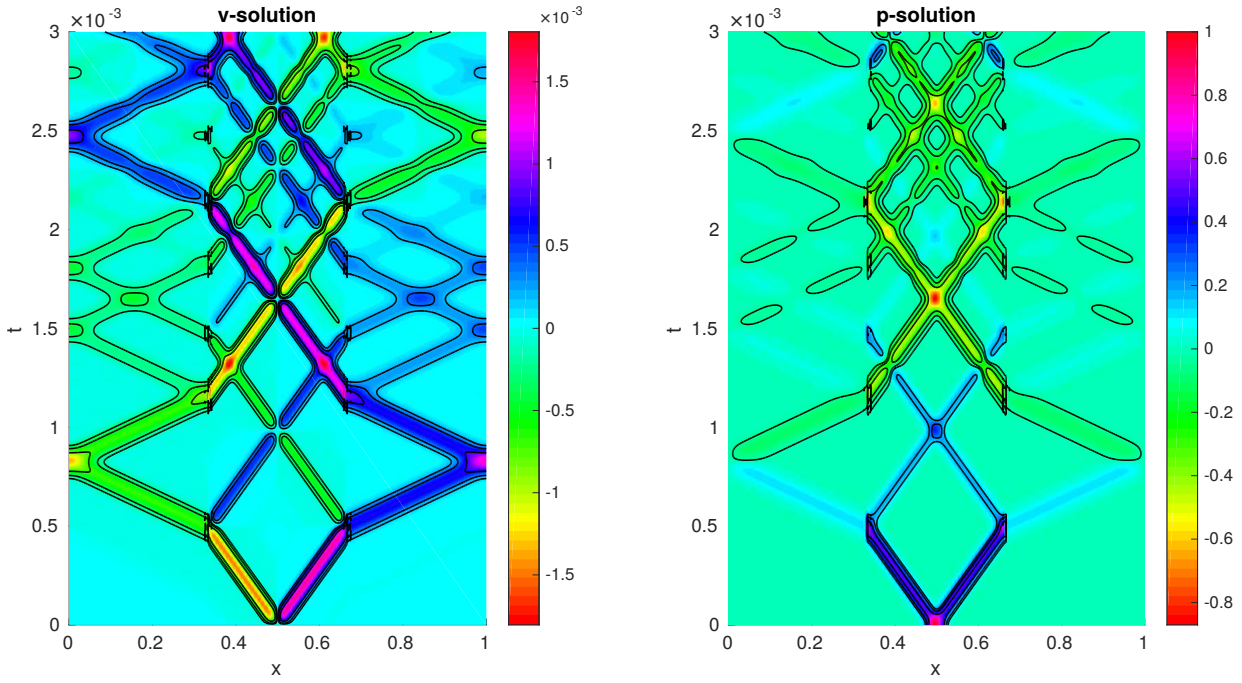

Figure 12: Setup as described in Figure 11 with dirichlet boundary conditions. The x-axis shows the position, the y-axis the time. At the jump, one can observe, that the wave abruptly changes amplitude. This is due to the change in ρ. The higher c in the outer domain manifests itself in the kinks at $x = \frac{1}{3}$ and $x = \frac{2}{3}$. The v-solution shows anti-symetry, whereas the p-solution is symmetric. 120 elements with a polymomial degree of 4 were used.

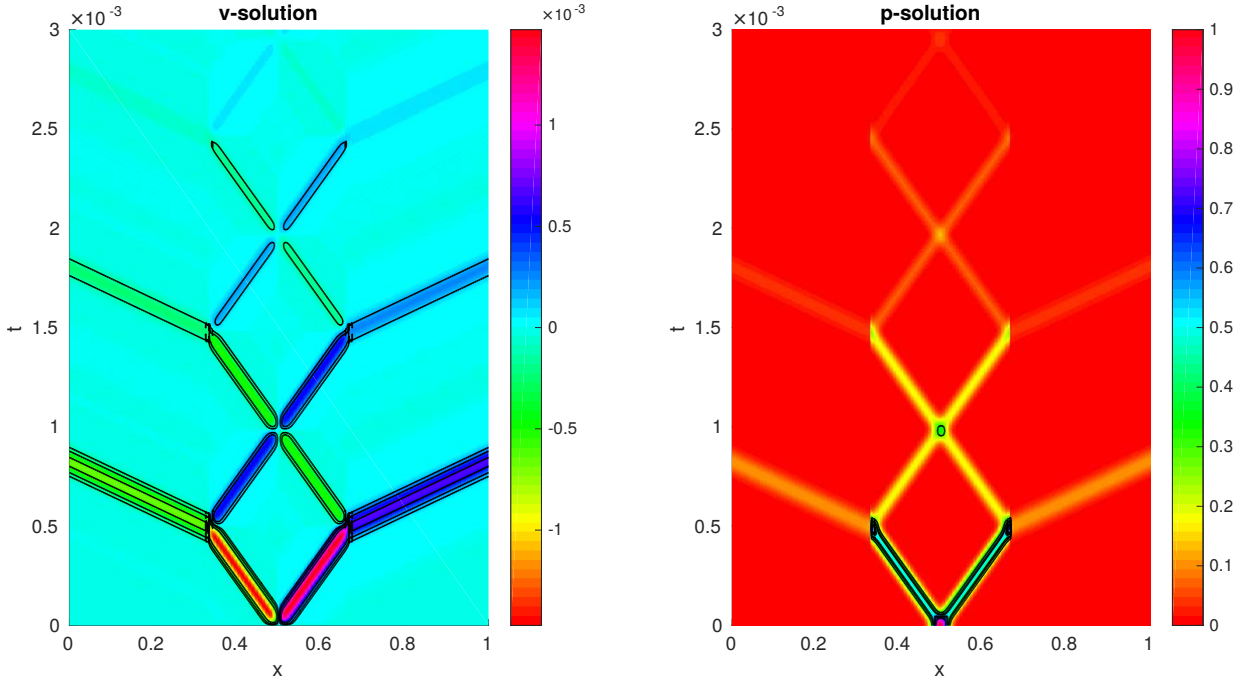

Figure 13: Setup as described in Figure 11 with absorbing boundary conditions. There are no signs of unwanted reflections at the boundary. 120 elements with a polymomial degree of 4 were used.